LA-UR- 96-4084

CONF-970201--11

Title: THERMAL AGING OF $LaNi_{5-x}Mn_x$ HYDRIDES

Author(s): S. Bagchi, D. Chandra, W. N. Cathey, University Of Nevada
R. C. Bowman Jr., California Institute Of Technology
Ricardo B. Schwarz, CMS
F. E. Lynch, Hydrogen Components Inc.

Submitted to: TMS Annual Meeting
TMS
February 9-13, 1997
Orlando FL

Los Alamos
NATIONAL LABORATORY

Form No. 836 R5
ST 2629 10/91

THERMAL AGING OF $LaNi_{5-x}Mn_x$ HYDRIDES

S. Bagchi, D. Chandra, W. N. Cathey
MS 170, University of Nevada, Reno, NV 89557-0136

R. C. Bowman Jr.
California Institute of Technology, Mail Stop 138-78, Pasadena CA 91702

R. B. Schwarz
Los Alamos National Laboratories, K765, Los Alamos NM 87545

and

F. E. Lynch
Hydrogen Components Inc., 12420 N. Dumont Way, Littleton CO 80125

Abstract

The $LaNi_{5-x}Mn_x$-hydrides have potential applications in cryocooling devices for non-mechanical method to compress hydrogen gas. Thermal aging behavior of $LaNi_{5-x}Mn_x$-hydrides of compositions x=0.4 and x=1.5 has been investigated. The hydriding properties of the $La_{1.02}Ni_{4.6}Mn_{0.4}$ alloy do not change significantly after thermal aging at 453K for 260 hours. X-ray diffraction analyses of this aged alloy do not reveal the presence of any new phases but the Bragg peaks become broader. Line profile analyses show anisotropic microstrains with an average $\langle e^2 \rangle^{1/2}$ value of ~5×10^{-3}. Thermal aging of the other hydride, $LaNi_{3.5}Mn_{1.5}$ hydride, at 623K for 280 hours, showed significant disproportionation; the hydrogen capacity reduced significantly from an H/M value of 0.75 in the activated condition to ~0.15 after aging. X-ray diffraction analyses showed disproportionated lanthanum dihydride, metallic Ni, and Mn phases. The Bragg peaks were very broad indicative of microstrains or small crystalline domains.

Proceedings of the Conference on "Rare Earths: Science, Technology, and Applications", 1997 TMS Annual Meeting, Orlando Florida, February 9-13, 1997. Edited by R. G. Bautista (TMS, Warrendale, Pa , 1997).

Introduction

The substitution of manganese for nickel in the rare earth intermetallic compound $LaNi_5$ provides flexibility for adjusting the plateau pressure for hydrogen absorption/desorption. It further decreases the propensity of disproportionation of the parent $LaNi_5$ intermetallic following cyclic hydriding/dehydriding [1-3]. Lartigue et al. [4] determined the thermodynamic properties of the $LaNi_{5-x}Mn_x$-H system and demonstrated whilst Mn additions lower the plateau pressure, it does not decrease significantly the hydrogen storage capacity. The crystal structure measurements of Percheron-Guégan et al. [5] for the $LaNi_{5-x}Mn_x$ system showed that the unit cell volume increase with increasing Mn and suggested that the Mg substitutes for nickel both in the 3g and 2c lattice positions. These authors further suggested that because (a) these alloys can be easily handled, (b) their plateau pressures can be easily tailored, and (c) they have high absorption/desorption capacity, $LaNi_{5-x}Mn_x$ should be ideal media for tritium storage. Ide et al. [6] and Limacher et al.[7] evaluated the aging of $LaNi_{5-x}Mn_x$ tritide at room temperature. The formation of helium leads to a lowering of the plateau pressure and a reduction in the capacity. Luo et al. [8] determined thermodynamic properties of the $LaNi_{5-x}Mn_x$-H system and resolved discrepancies in published data [9]. From their data one can infer that the top of the miscibility gap in the metal/hydrogen phase diagram occurs at a temperature of approximately 675 K and an H/M value of 2.5.

A major consideration in the use of rare-earth alloys for hydrogen storage is the long-term stability of the material. The stability of hydrogen storage materials has been investigated following two approaches: (1) *cyclic aging,* consisting in measuring the hydrogen storage capacity after repetitive hydrogen uptake and discharge cycles, [8], and (2) *thermal aging,* consisting in measuring the storage capacity following long-term exposure to hydrogen at a temperature usually higher than that of service [10,11]. These two approaches have been demonstrated to be somewhat equivalent [11]. Thermal aging, however, has the advantage that it allows for a faster assessment of the alloy stability. When the alloy is unstable, both testing methods can lead to disproportionation, which is manifested by changes in the shape of the isotherms and/or loss of hydrogen storage capacity. Lambert et al. [11] have shown that the disproportionation occurring during either cycling or thermal aging is accompanied by the development of large residual microstrains. Sandrock [10] showed that vacuum annealing tends to restore the disproportionated materials to their original condition.

In this paper, we use the thermal aging method to study the stability of hydrides of $LaNi_{5-x}Mn_x$. Two compositions, $x = 0.4$ and $x = 1.5$, were chosen for their potential use in Joule-Thomson cryogenic refrigerators, heat pumps, and tritium storage. Pressure-composition isotherms were measured before and after thermal aging and the changes in properties were evaluated using the thermodynamic data of Luo et al.[8]. X-ray diffraction was used to detect the appearance of new phases due to disproportion and to measure the microstrains. Large-scale solute segregation as the result of disproportionation was also studied by chemical analysis in the scanning electron microscope.

Experimental Procedures

The $LaNi_{4.6}Mn_{0.4}$ alloy was prepared at Hydrogen Components Inc. (HCI) by arc-melting the elements (better than 99.5% purity), using the method described by Lambert et al. [11]. This alloy was annealed in high-purity argon at 1473°C for 24 hours. The $LaNi_{3.5}Mn_{1.5}$ intermetallic was provided by Aerojet Corporation. It was prepared at the Ames Laboratory of Iowa State University from 99.9+ % purity elements; this alloy was annealed at 1073K for seven days [8]. X-ray powder diffraction analyses showed that these two compounds were single-phase. The sharp Bragg peaks indicated no residual strain in the samples in as-annealed condition.

Pressure-composition isotherms and thermal aging studies were made at the University of Nevada, Reno, in a Sievert's apparatus . A tubular furnace was used to heat the sample and the temperature was controlled to within ±1°C by a Omega type CN 7000 PID controller. For the thermal aging studies, the samples were pressurized by hydrogen (UHP grade) and changes in the pressure were recorded by a strip chart recorder.

Two x-ray powder diffraction systems were used for structural analyses. A Nicolet-Siemens automated powder diffractometer using Cu Kα radiation was used for the majority of the work. Quartz capillaries were used to hold the hydride powder samples, which were sealed with epoxy. Four capillaries were placed coplanar onto a glass slide to approach a Bragg-Brentano diffraction geometry. A Scintag diffractometer equipped with a Peltier-cooled solid-state detector was used at the Los Alamos National Laboratory to determine the microstrains and domain sizes. In this case, the intermetallic powder were placed on a low-background quartz single-crystal substrate. The Bragg peak profiles were fitted by a modified Pearson-VII function to determine their integral breadth. Wherever possible, a small amount of Si standard (NBS 640b) was added to the samples to correct for instrumental shift errors.

The Scintag instrumental peak broadening was measured with NBS LaB_6 standard. The integral breadths (β) of the sample Bragg peaks were obtained after deconvulting any overlapping peaks and correcting for instrumental peak broadening according to the method described by Aqua [12]. Microstrains and crystallite sizes were determined using the following equation [12,13]:

$$(\beta \cos\theta / \lambda)^2 = 1/D^2 + 16\, e \sin\theta / \lambda)^2 \qquad (1)$$

where, θ is the Bragg angle, λ is the wavelength of the x-rays, e is the strain, and β is the true integral breadth obtained using the following equation:

$$\beta / B = 1 - (b^2 / B^2) \ . \qquad (2)$$

In the above equation, B is the measured profile breadth and b is the instrumental profile breadth, both measured at the same diffracting angle. The rms strain, $\langle \varepsilon^2 \rangle^{1/2}$, may be evaluated by the formula:

$$\langle \varepsilon^2 \rangle^{1/2} = 1.25\, e \qquad (3)$$

Scanning electron microscopy (SEM) analyses were made using a JEOL-840A SEM at the University of Nevada, Reno. Standard procedure of sputtering a thin film of Au-Pd alloy was used to make the samples conductive. A Kevex energy dispersive analyzer capable of detecting C, O, and N was used for semiqauntitative analyses.

Results

Thermal Aging of $La_{1.02}Ni_{4.6}Mn_{0.4}$

After aging $LaNi_{4.6}Mn_{0.4}$ hydride at 453 K and a pressure of 1378 kPa for 260 hours, the alloy showed no disproportionation. Figure 1 shows pressure-composition isotherms taken before and after aging at the temperature of 323 K (i.e., lower than the aging temperature). The isotherms before aging were taken in the conventional manner, i.e., the absorption isotherm was measured first, followed by the desorption isotherm. Following the aging, the temperature was decrease to 323 K and the isotherms were taken in the reverse order, i.e., the desorption isotherm was measured first. It is clear that aging causes little decrease in the plateau pressures. The desorption isotherm for the aged alloy does not reach a zero H/M value indicating that the alloy trapped hydrogen most likely as an absorbed layer. The amount of hydrogen absorbed is likely to increase with the communition of the particles caused by volume changes during hydriding.

The x-ray diffraction patterns in Figure 2 were all obtained from $La_{1.02}Ni_{4.6}Mn_{0.4}$ alloy after the aging test. Curve (2a) is for the hydride in the as-aged state, while still in the beta-phase under an hydrogen pressure. This data was acquired with a sample aliquot inside a fused silica capillary which contributed to the high background at small scattering angles. Silicon powder (NBS standard No. 640B) was mixed with the sample powder. The Bragg peaks in this pattern match those of the hydride β phase of $La_{1.02}Ni_{4.6}Mn_{0.4}$ with no detectable α phase. Curve (2b)

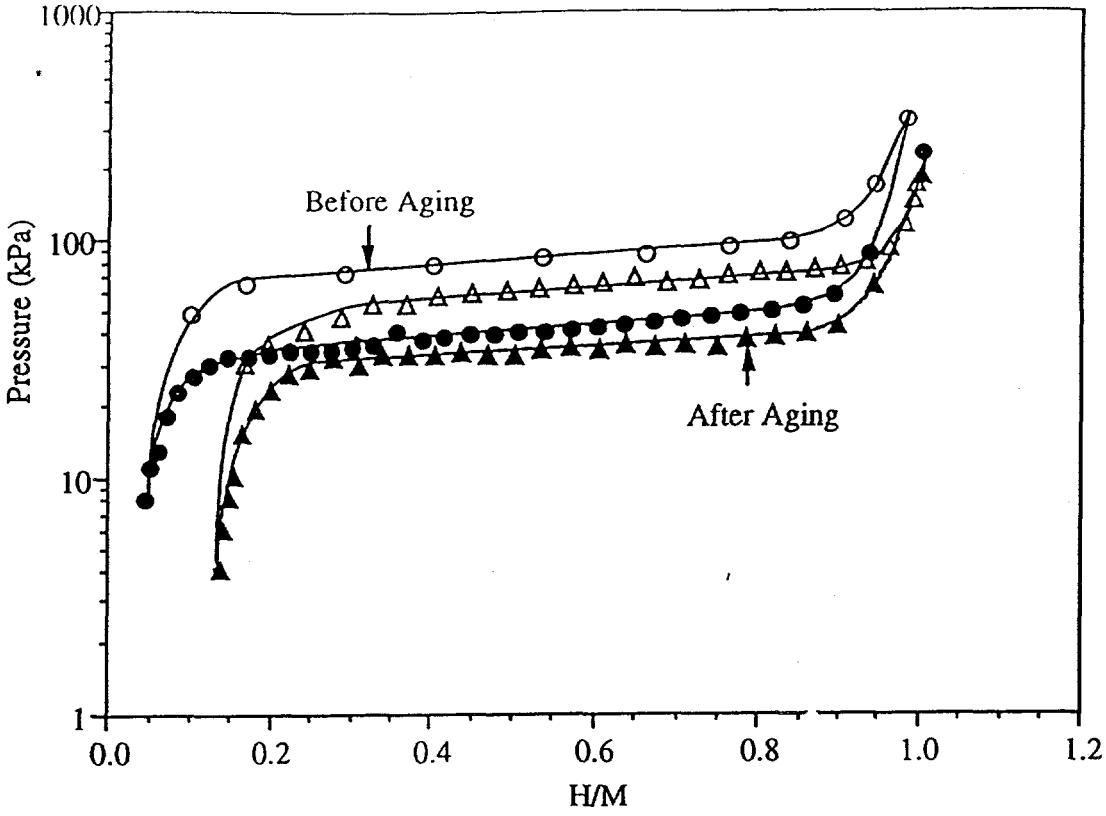

Figure 1. Pressure-composition isotherms of $La_{1.02}Ni_{4.6}Mn_{0.4}$ taken at 323 K before and after thermal aging at 453 K for 260 hours.

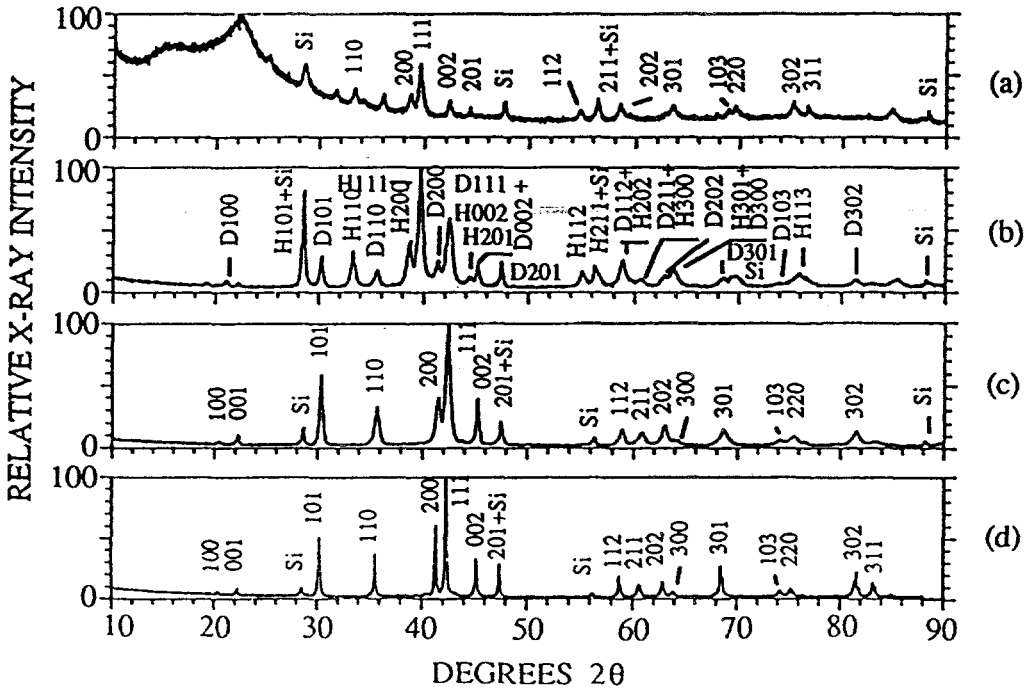

Figure 2. X-ray diffraction patterns of $La_{1.02}Ni_{4.6}Mn_{0.4}$ in (a) aged and in the hydrided condition (sample in quartz capillary) (b) aged and partially desorbed (c) aged and fully desorbed and (d) aged and then annealed.[4] The "H" denotes peaks of the β phase and "D" those of the α phase.

was obtained immediately after breaking the capillary and exposing the hydride to air. Since the plateau pressure at room temperature is about 20 kPa, and the partial pressure of hydrogen in the atmosphere is negligible, after removing the hydrogen over-pressure the alloy should reverse to the α phase. However, for short times, most of the alloy remains in the beta phase. The pattern shows both α and β phases. Bragg peaks form the β phase have been identified by the letter D. Curve (2c) is a pattern taken on the same alloy after exposing it to air for two weeks. All the Bragg peaks in the patterns correspond to the α phase. Both curves (2b) and (2c) show relatively broad Bragg peaks which indicate either small crystalline domains and/or the presence of microstrains in the sample. Curve (2d) was obtained after heating the sample in vacuo at 1448K for 16 hours. All the Bragg peaks correspond to $La_{1.02}Ni_{4.6}Mn_{0.4}$ and the peaks are now sharp. This sequence of diffraction patterns confirm the conclusions drawn from the isotherms, namely that aging $La_{1.02}Ni_{4.6}Mn_{0.4}$ in the hydride state causes no observable disproportionation and the alloy retains its hydrogen storage properties.

Thermal Aging of $LaNi_{3.5}Mn_{1.5}$

Luo et al. [8] showed that the $LaNi_{3.5}Mn_{1.5}$-H system has a miscibility gap with a critical temperature of ~675 K, above which the hydride is unstable. After reaching the mid-plateau region at 623K (approximately 50 K below the critical point), the authors interrupted the data acquisition for 12 hours. The subsequent desorption isotherm had a very steep slope which the authors took as an indication of sample degradation during aging.

In this study, thermal aging of $LaNi_{3.5}Mn_{1.5}$ was performed for 280 hours at 623K. Figure 3 shows the isotherms taken at 473K before and after the aging treatment. In contrast with the results for the $La_{1.02}Ni_{4.6}Mn_{0.4}$, the $LaNi_{3.5}Mn_{1.5}$ alloy shows a large degradation in its hydrogen storage capacity, which decreased sharply from 0.75 before aging, to approximately ~0.15 after aging. The x-ray diffraction patterns of $LaNi_{3.5}Mn_{1.5}$ (after aging) are shown in Figure 4. Curve (a) was obtained after removing the sample from the high-pressure hydrogen gas and exposing it to air. The pattern showed very broad Bragg peaks which made it difficult to identify the phases present in this alloy. In an attempt to identify these phases, we also analyzed

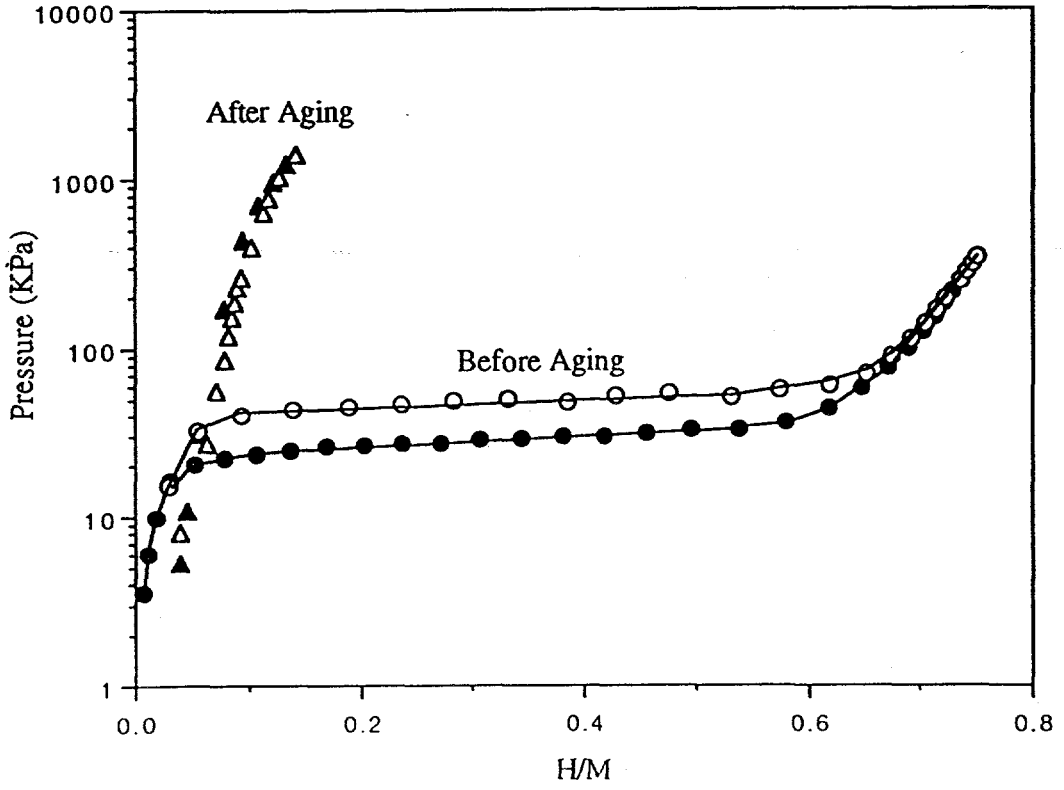

Figure 3. Pressure-composition isotherms of $LaNi_{3.5}Mn_{1.5}$ taken at 473 K before and after thermal aging at 623 K for 280 hours.

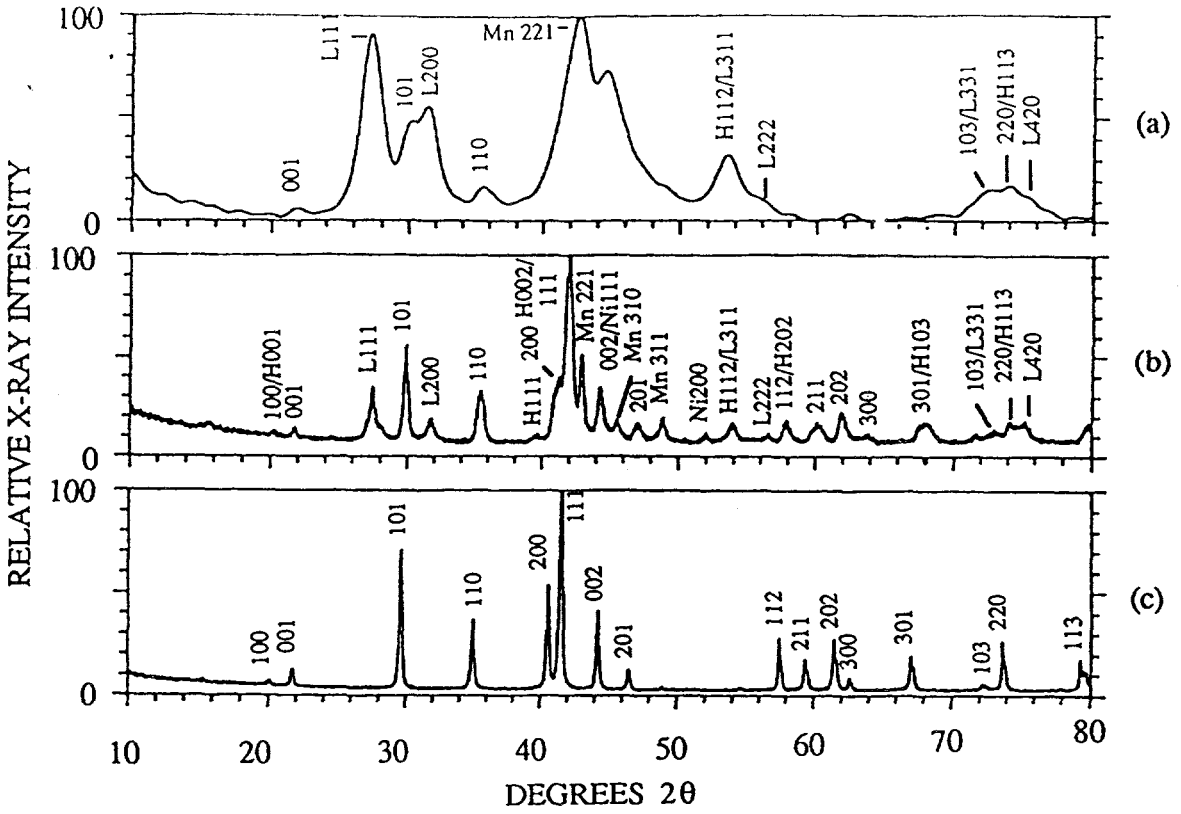

Figure 4. The X-ray diffraction patterns of $LaNi_{3.5}Mn_{1.5}$ (a) after 280 hours aging at 623K (b) after 12 hours aging at 623K and (c) annealed alloy. The "H" refers to β phase and "L" to LaH_2 phase.

the sample used by Luo et al.[8] which was exposed to hydrogen for ~12 hours at 623K. We will refer to it as the "12 hour aged" sample. The diffraction pattern of this sample, shown in curve (b) shows, in addition to the expected Bragg peaks of the α- and β-phases of $LaNi_{3.5}Mn_{1.5}$-H_X, peaks corresponding to LaH_2, Ni, and Mn. Clearly, the "12 hour aged" alloy disproportionated during the aging treatment. Curve (c) is a diffraction pattern from the $LaNi_{3.5}Mn_{1.5}$ sample taken after vacuum annealing at about 1400 K for 16 hours. The high temperature annealing restores the equilibrium compound.

The SEM observations revealed extensively fractured particles which is typical of hydrided particles. Following fracturing, the particles sizes range from about 5 to 30 μm (Figure 5). An energy dispersive x-ray analysis of thermally aged samples revealed that the majority phase was $LaNi_{3.5}Mn_{1.5}$. Embedded within the $LaNi_{3.5}Mn_{1.5}$ domains were regions rich in lanthanum, only 1 to 5 μm in size. These particles were easy to detect because they appeared brighter than the $LaNi_{3.5}Mn_{1.5}$ phase. Figure 6 shows x-ray intensities measured in the $LaNi_{3.5}Mn_{1.5}$ phase (A) and in the brighter regions (B). The scales in these two figures do not correspond. From Figure (B), we infer that the bright regions have a composition close to $La_x(Ni, Mn)_{1-x}$, where x >0.95. In this type of analysis, the signal from the bright regions includes also x-rays scattered from adjacent regions, which may contain Ni and Mn. The data suggests, however, that the bright regions are LaH_2 that formed by a disproportionation of the $LaNi_{3.5}Mn_{1.5}$-H_X alloy.

Lattice Parameters of the Alloys

The substitution of nickel by the larger manganese atoms causes a lattice expansion in $LaNi_5$. Table 1 gives the lattice parameter, the c/a ratio, and the cell volume of the various alloys studied in this work, measured by x-ray diffraction. The β–phase hydride showed almost isotropic increases of 6.6% and 6.3% in a- and c-directions, respectively. After desorbing, the α–phase developed long range strains; the lattice contracted by -0.14% in the a-direction and expanded by +0.17% in the c-direction after aging.

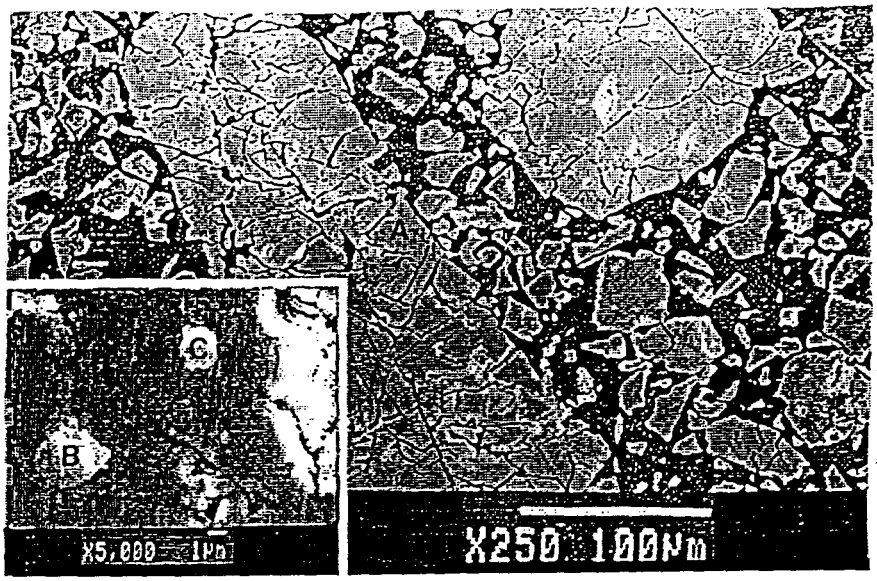

Figure 5. Scanning electron micrograph of fragmented particles of $LaNi_{3.5}Mn_{1.5}$. The inset, taken at 5000x, shows lanthanum-rich domains formed by the disproportionation of the alloy during aging (particles B and C) .

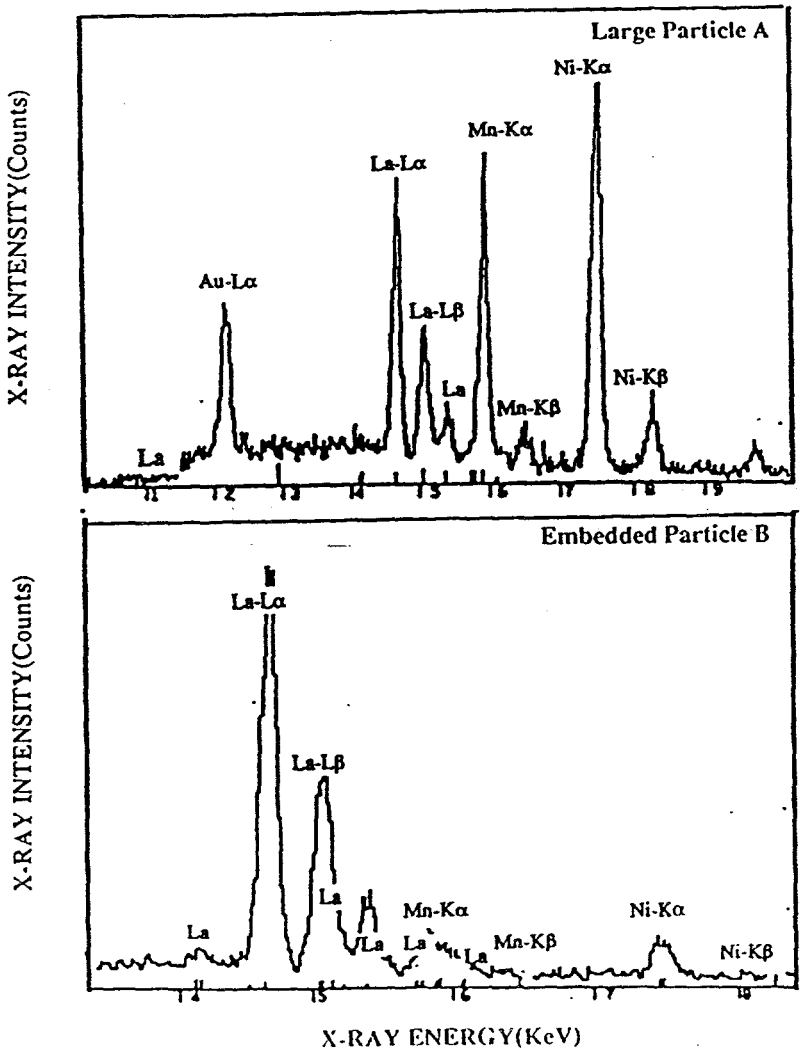

Figure 6. Energy dispersive spectrum of particle A in Figure 5 (top), having a composition close to $LaNi_{3.5}Mn_{1.5}$. Spectrum from a bright region (B) within the particles (bottom).

Table I. Lattice Parameters of $La_{1.02}Ni_{4.6}Mn_{0.4}$ in the annealed, hydrided, and desorbed conditions after thermal aging. The thermal aging was performed at 453 K for 260 hours. Lattice parameters reported by Buschow and van Mal [16] for annealed $LaNi_5$ are also listed for comparison. Standard deviations are listed in parentheses.

MATERIAL	LATTICE PARAMETERS			
	a (Å)	c(Å)	c/a	Cell Volume (Å^3)
1. $La_{1.02}Ni_{4.6}Mn_{0.4}$ (α phase-annealed)	5.0481 (0.0014)	4.0110 (0.0009)	0.795	88.5
2. $La_{1.02}Ni_{4.6}Mn_{0.4}$ (β phase)	5.4075 (0.0042)	4.2849 (0.0025)	0.792	108.5
3. $La_{1.02}Ni_{4.6}Mn_{0.4}$ (α phase after aging)	5.0410 (0.0038)	4.0180 (0.0026)	0.798	88.4
4. $LaNi_{3.5}Mn_{1.5}$ (α phase after aging)	5.1341 (0.0026)	4.0993Å (0.0015)	0.798	93.6
5. $LaNi_5$ [16] (α phase-annealed)	5.017	3.987	0.795	86.9

Residual Strains in the α phase After Aging

The Bragg peaks of the aged alloys show significant broadening. The data for the β phases of the $LaNi_5$-xMn_x with x = 0.4 and x = 1.5 (curves (a) in Figs. 2 and 4) did not allow us to separate the contributions to the broadening arising from the crystallize size and the microstrains. This analysis was however performed on the aged alloys after being desorbed back into the α phase. Figure 7 shows a $(\beta \cos\theta / \lambda)^2$ vs $(\sin\theta / \lambda)^2$ plot for aged $La_{1.02}Ni_{4.6}Mn_{0.4}$ obtained from the diffraction pattern shown in Figure 2c. In such a plot, the data points tend to lie in a straight line; then, the intercept on the abscissa yields the size of the crystalline domains which diffract coherently, whereas the slope of this line yields the root-mean squared value of the fluctuating microstrain within these domains. The solid line in Figure 7 is the best fit to all the data and predicts a crystalline domain size of 52 nm and a microstrain of about 0.05%. This data shows considerable scatter. We found, however, that the scatter is significantly smaller if the data are grouped according to their Miller indices. Although the grouping is not perfect, overall the grouping indicated that reflections of the type (h00) and (hk0) had significantly higher residual strains than reflections of the type (00l). Figure 8 shows the corresponding analysis of the x-ray data for the $LaNi_{3.5}Mn_{1.5}$ alloy. In this case, all the diffraction peaks can be adequately fitted by a single strait line. The intercept and slope of this line give a coherent crystallite domains of 32 nm and a residual strain of 0.058%. These results agree with earlier diffraction data of Percheron-Guégan et al [5] on $LaNi_{5-x}Mn_x$ alloys which showed that the anisotropy in the microstrain is larger in alloys of low manganese content. It should be noted that the microstrains in the (00l) direction of hydrided and desorbed $LaNi_5$ is almost zero [5]. Currently, there is no conclusive interpretation for this effect.

Figures 7 and 8 show that annealing the aged sampled leads to an increase in the size of the crystallite domains and an almost total elimination of the residual strains.

Discussion

From this study, it is clear that the stability of $LaNi_{5-x}Mn_x$ alloys aged in the β phase depends critically on the value of x. The alloy with x ~ 0.4 is quite stable whereas the alloy with x ~ 1.4 disproportionates readily. In the case of $La_{1.02}Ni_{4.6}Mn_{0.4}$, thermal aging causes a small decrease in plateau pressures (Figure 1). Lambert et al. [11] and Chandra et al. [15] observed a lowering of the plateau pressures in $LaNi_{4.27}Sn_{0.24}$ and $LaNi_{4.25}Al_{0.75}$ following aging. It is interesting to note that a similar lowering of plateau pressure has been observed in $LaNi_{5-x}Mn_x$ intermetallics loaded with tritium and aged at room temperature. Limachar et al. [7] and Nobile et al. [14] attributed the lowering of the plateau pressures to volume increases caused by trapped interstitial ^3He [7] or to hydrostatic stresses induced by ^3He bubbles which form in the alloy with increased aging times. Obviously, this does not explain the lowering of the plateau pressures in the present alloys but it suggests that the residual anisotropic microstrains could be contributing to the lowering of plateau pressure.

The observed difference in the stability of the $LaNi_{5-x}Mn_x$ alloys with x = 0.4 and x = 1.5 is so large that it is unlikely that it was caused by to the difference in the aging temperatures, 453 K and 623 K. If the disproportionation is caused by micro-strains in the lattice, then it is likely that the disproportionation will be more severe as one approaches the critical point in the metal-hydrogen miscibility gap. The critical point is characterized by large fluctuations in the local hydrogen concentration and this should result in large micro-strains. In comparing the disproportionation of different alloys, it is thus important to perform the aging at temperature, composition, and pressure conditions which are the same fraction of these values at the corresponding critical points. The temperature at the critical point of the x = 1.5 alloy was estimated at 675 K. To our knowledge, there is no data to estimate the temperature at the critical point of the x = 0.4 alloy. At one atmosphere hydrogen, the plateau temperature of the x = 0.4 alloy is about 330 K whereas for the same pressure the x = 1.5 alloy has a plateau temperature of 500 K. This suggests that the temperature at the critical point of the x = 0.4 alloy is somewhat lower than that of the x = 1.5 alloy. The difference in critical temperatures is in the direction needed to have a similar ratio of aging temperature to critical temperature.

The disproportionation of the $LaNi_{5-x}Mn_x$ with x~1.5 leads to the formation of pure La or a La-rich phase. In the presence of impurities, this phase can easily react to form an oxide. Both phases are very stable and once formed, no longer contribute to the reversible hydrogen storage.

Conclusions

The intermetallic $La_{1.02}Ni_{4.6}Mn_{0.4}$ does not disproportionate after thermal aging at 623K for 260 hours. The hydrogen capacity decreases by about 10%. There is also a slight decrease in the plateau pressures. Anisotropic lattice micro-strains were detected in the aged $La_{1.02}Ni_{4.6}Mn_{0.4}$ alloy similar to those reported by Percheron-Guégan [5] for activated $LaNi_{5-x}Mn_x$ ($0.05<x<0.5$).

Upon aging, $LaNi_{3.5}Mn_{1.5}$ showed extensive disproportionation with a significant loss in hydrogen capacity. The isotherm of the aged alloy showed no plateau. Aging resulted in partial disproportionation of $LaNi_{3.5}Mn_{1.5}$ hydride to $La_x(Ni,Mn)_{1-x}$ H_2, Ni and Mn. Large lattice micro-strains produced extensive broadening of the Bragg peaks. The extent of disproportionation was also apparent in a sample aged for only 12 hours.

Acknowledgment

This work was supported by Aerojet Corporation, Azusa CA.

References

1. J. C. Archard, A. Percheron-Guegan, H. Diaz, F. Briaucourt and F. Demeny, 2nd International Congr. on Hydrogen in Metals, (Paper #1E12) Paris, June 1977.

2. Percheron-Guégan, J. C. Archard, J. Saraddin, and G. Bronoel, in A. F. Anderson and A. J. Maeland (eds.), Proc. Int. Symp. on Metal Hydrides for Energy Storage, Gelio, August 2977, Permagon Press, Oxford, (1978) 485.

3. F. E. Lynch, J. Less-Common Met., 172 (1991) 943.

4. A. Lartigue, A. Percheron-Guégan, J. Archard and F. Tasset, J. Less-Common Met, 75 (1991) 23.

5. A. Percheron-Guégan, C. Lartigue, J. C. Archard and P. Germi, F. Tasset, J. Less-Common Met, 74 (1980) 1.

6. T. Ide, F. Sakai, M. Yorozu, K. Hirata, J. Mitsui, H. Yoshida and Y. Naruse, Fusion Tech., 14 (1988) 769.

7. B. Limacher, D. Leroy, C. Arnaux, F. Gaspard, *J. Alloys Comp.*, 321(1995) 792.

8. W. Luo, S. Luo, J. D. Clewely, T. B. Flanagan, R.C. Bowman.Jr, J.S. Cantrell, J. Alloys Comp., 202 (1993) 147.

9. J. Murray, M. Post and J. Taylor, in T. N. Veriroglu (ed.) Metal Hydrogen Systems, Pergamon Press, New York (1982) 445.

10. G. Sandrock, , P. Goodel, , E. Houston, and P. Golben, Z. Physik. Chem, NF., 164 (1989) 103

11. S.W. Lambert, D. Chandra, W.N. Cathey, F. E. Lynch and R.C. Bowman, J. Alloy and Compounds, 187 (1992) 113.

12. N. Aqua, Acta Cryst., 20, (1966) 560.

13. T. R. Anantharaman and J. W. Christina , Acta Cryst., 9, (1956) 479.

14. A. Nobile, Jr., R.T. Walters and W.C. Mosely, J. Less-Common Met. 172-174 (1991) 1352.

15. D. Chandra, W.N. Cathey, H. Mandalia, J. R. Wermer, J. S. Holder, Paper No. M4 -10P presented at The International Symposium on Metal Hydrogen Systems, Les Diablerets, Switzerland (Aug 25-30, 1996).

16. K. H. J. Buschow and V. H. van Mal, J. Less-Common Met., 29 (1972) 203.

DISCLAIMER